Journal of Engineering Science and Technology
Vol. 12, No. 8 (2017) 2238 - 2253

LASER POINTER DETECTION BASED ON INTENSITY PROFILE ANALYSIS FOR APPLICATION IN TELECONSULTATION

NAIREEN IMTIAZ, MOHD MARZUKI MUSTAFA*,
AINI HUSSAIN, EDGAR SCAVINO

Department of Electrical, Electronic and Systems Engineering,
Universiti Kebangsaan Malaysia, Bangi, Selangor, Malaysia
*Corresponding Author: marzuki@ukm.edu.my

Abstract

Telemedicine is application of electronic communication to deliver medical care remotely. An important aspect of telemedicine is teleconsultation which involves obtaining the professional opinion of a healthcare provider. One of the ways to improve teleconsultation is to equip the remote specialist via control of a laser pointer, located in the consultation area to provide a means of gesture. As such, accurate detection of laser spot is crucial in such systems as they rely on visual feedback, which enables the specialist in a remote site to control and point the laser in the active location using a standard mouse. The main issue in laser spot detection in a natural environment is the distinguishability of a laser point image from other bright regions and glare due to camera saturation. This problem remains unsolved without extensive computing and use of hardware filters. In this paper a hybrid algorithm is described which is aimed to work with natural indoor environment while limiting computation. This algorithm combines thresholding and blob evaluation methods with a novel image intensity profile comparison method based on linear regression. A comparison of the algorithm has been done with existing approaches. The developed algorithm shows a higher accuracy and faster execution time making it an ideal candidate for real time detection applications.

Keywords: Teleconsultation, Laser pointer detection, Blob management, Profile matching, Image processing.

1. Introduction

Electronic communication technology based remote medical practices are characterized as telemedicine [1]. Telemedicine has the potential to be an effective tool in improving health standards by providing specialised assistance in

Nomenclatures

A	Area, m^2
BA	Blob area threshold
BC	Blob circularity
DU	Dynamic umbralization
f_i	Predictive model line
FN	False negative outcome
FP	False positive outcome
LR	Linear regression
P	Perimeter, m
r^2	Regression value
SS_{res}	Residual sum of squares
SS_{tot}	Total sum of squares
T	Intensity threshold
TM	Template matching
TN	True negative outcome
TP	True positive outcome
y_i	Data points

Abbreviations

BD	Bhattacharya distance
CSCW	Computer supported cooperative work
ED	Euclidean distance
HSV	Hue saturation value
MATLAB	Matrix laboratory
MP	Mega pixels
NCC	Normalized cross correlation
RGB	Red green blue
ROI	Region of interest
SD	Standard deviation

less accessible areas. It assures better healthcare in situations where medical services cannot be promptly provided [2, 3]. Many developing nations have a large number of remote regions that can benefit greatly from telemedicine services [4]. One of the aspects of telemedicine is Teleconsultation. Teleconsultation is a clinical discussion that takes place remotely using the concept of computer-supported cooperative work (CSCW) [5]. Means to provide gesture to the remote specialist are being researched to increase the effectiveness of services by allowing a remote specialist to draw attention to precise areas [6]. A laser pointer assisted system is an example of such a system in which a mouse pointer positioned on screen translates into laser movement on the remote site.

Figure 1 describes a typical teleconsultation setup incorporating a laser pointer. The remote specialist receives live image over the internet from the local site. He uses a mouse to move a pointer on the screen to desired location on the image. At the local site, a laser pointer moves to point to the same location on the patient body. This setup removes the need for the medical person at local site to look at a screen hence maintaining his focus.

Positioning the laser pointer to the desired location can be done by calibrating the pointer but this will make the system sensitive to the relative position of the laser pointer and patient. The systems that use laser pointers rely on visual feedback as described in Fig. 1(b) [6]. The client PC provides the target coordinates for the laser pointer location. In order to ensure that the laser moves to the correct location on the clinical site as that described by the pointer on the client PC, a feedback is essential. This feedback system is required to detect the laser pointer in order to compare it with the input coordinate and apply the appropriate control action to reduce the error if any.

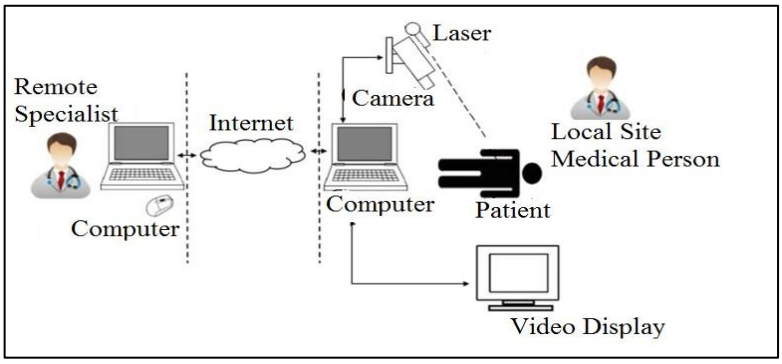

(a)Typical system overview.

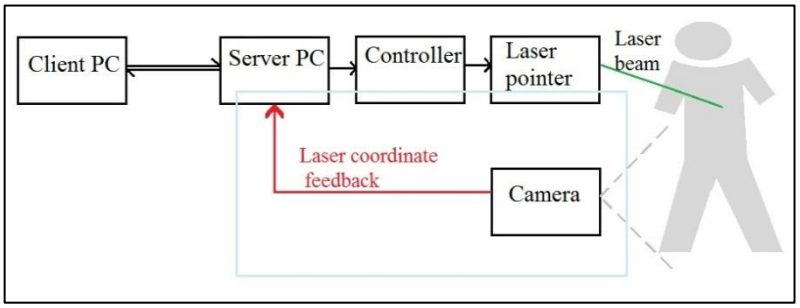

(b) Laser pointer feedback control loop.

Fig. 1. Laser pointer system applied in teleconsultation.

The main issue in implementing the visual feedback for controlling the laser pointer is that the laser pointer in camera images is not always distinguishable from other bright regions due to glare caused by bright lights oversaturating the camera. Many existing laser spot detection algorithms work in controlled environments as they focus on implementing laser pointer interaction with display screens. These approaches are unsuitable for practical teleconsultation environments where natural surfaces, small objects, etc. reflect light and form glare. Existing algorithms [7 - 9] that work with slightly less controlled environment are appropriate only for stationary images, having no error caused by temporal laser movement. Moreover, they rely on computationally extensive processes which are impractical to use with continuous video frames.

The detectability of the laser which seems like a trivial task is a complex problem and is amplified by the computational time and process cost constraints.

In this paper a laser pointer detection algorithm is developed which has a high accuracy in natural indoor environment while limiting the process computational time and cost. This algorithm combines simple image processing techniques aimed to extract the position by utilizing all laser pointer features known and uses linear regression analysis as a final classifier for position identification in live camera images.

Section 2 of this paper gives a brief overview of the existing approaches to detect laser pointer from images. In Section 3, the algorithm overview as well as the details of all the steps involved are shown. Specifics of the conducted experimentation are given in Section 4. Brief details of alternate methods used for comparison are also given. The results are presented and discussed in Section 5. Concluding points and research highlights are given in Section 6.

2. Existing research

Laser detection process seems simple but in reality is very complex due to a number of problems among which the most prominent is glare, i.e., light reflected from surfaces of objects. It is hard to distinguish from laser pointer in camera images. A simple one step detection algorithm is described in [10, 11], where the authors used color thresholding in HSV format. This method is limited to work only with images where background does not contain colors similar to the laser. The authors of [10] also provide an alternative method of background subtraction which works only with static background images as it relies on identifying change.

A two-step method using a color threshold and convolution filter is presented in [12]. Three-step algorithms are presented by [13 - 15]. In [13], areas of motion are detected by background subtraction. In these regions laser image and histogram are compared using convolution. Centroid of the best matched region is taken as laser spot. The authors in [14] use thresholding to obtain a binary image followed by blob management. The authors state that the brightness of laser must be higher than surroundings. This limitation fails to accommodate the challenge of glare. In [15] adaptive threshold is applied on HSV Image to obtain a binary image. Blob management is performed by comparison with prior area and circularity information. The final laser classification is done on the bases of comparing mean of the spot region hue value.

A few algorithms also use hardware modification to enhance detection. Work reported in [16] uses a color filter and in [17] uses multiple camera results to consolidate and form one location. Frequency modulated laser pointer is used in [18] with a demodulating image sensor to retrieve laser location where as in [19] the author has used a blinking laser.

Some algorithms combine hardware and multi-step software methods. The study in [20] uses a camera filter to enhance laser pointer. A three step algorithm is described in [21] beginning with camera shutter rate, exposure setting followed by background subtraction. Another elaborate algorithm is described in [7] where camera exposure is adjusted based on V channel average value of an HSV image followed by a second threshold is applied on V channel to obtain blobs. Blob area to blob pixel area ratio is analyzed as well as color of the blob in original image frame using thresholds. Overall best is classified as laser spot.

Only few works are aimed to achieve detection in real indoor environments. [8, 9] present a three step algorithm using template matching and dynamic umbralization (TM+DU). Template matching best match is verified by dynamic threshold obtained using histogram properties [20, 21] also present an alternative method which uses the best match from template matching and a fuzzy rule base as a final laser classifier. The results of this algorithm are better than TM+DU but the whole process is computationally extensive for a video operation. The researchers in [22] use a monochrome camera with narrow bandwidth filter with a frequency that matches laser. Threshold is applied to shortlist laser pixels.

3. Methodology

Details of the developed hybrid algorithm are described in this section. The aim is to work with natural indoor environment and is fast enough to be used with video processing. The algorithm combines thresholding and blob evaluation methods with a novel profile analysis method based on linear regression. The developed algorithm focuses only on achieving a software solution to the detection problem as such if hardware adjustments are applied the detection may be further improved. The algorithm developed in this paper works in two stages.

- Segmentation
- Classification

Segmentation includes obtaining regions of interest (ROI) in three blob analysis based steps. This ensures that the algorithm is fast since blob analysis involves binary images and simple calculations. The intensity surface plane of ROI are analysed in the classification stage to match with a laser profile. These stages are discussed in detail in Sections 2.1 and 2.2.

Raw image frames have noise causing intensity surface roughness which affects the classification step as it depends on intensity profile of the image. In order to attenuate noise in the intensity surface, Gaussian smoothing filter is applied. This filter has a blur effect that results in a smooth intensity surface which makes profiles more comparable without loss of important image gradients. Over all detection process is shown in Fig. 2.

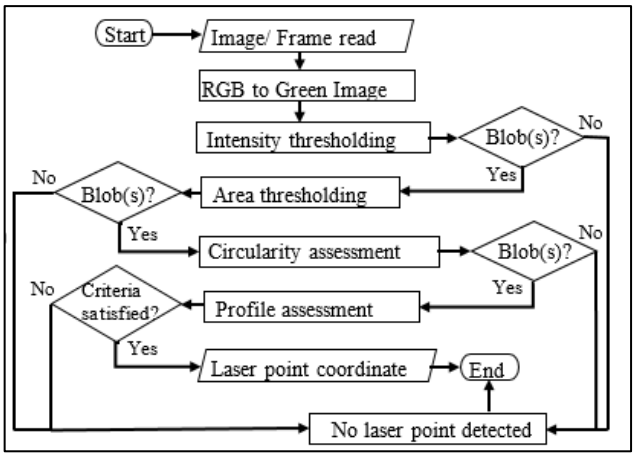

Fig. 2. Process flow chart.

3.1. Regions of interest (ROI) image

To obtain ROI, image details are reduced in steps leading to most likely area that may contain laser pointer. The laser color was arbitrarily chosen is green. Consequently using only green color channel subtracts features that are unlikely to be laser spot. Figure 3(a) shows an image with only green channel.

In the first step an intensity threshold (T) is applied on the green channel obtained in the previous step since laser pointer image pixels have high values due to extreme brightness. Based on repeated trial and error experiments with different sets of images the optimum value of this threshold is deduced to be 95 percent of maximum pixel intensity. Figure 3(b) shows the blobs obtained by thresholding. Binarization additionally reduces the runtime of the algorithm significantly.

In the second step a blob area threshold (BA) is applied in order to remove insignificant blobs as the binary image obtained may contain only a laser blob but generally this is not the case due to glare and bright regions of the image. Area of the blob that corresponds to laser pointer depends on the distance of the camera from the surface where the laser pointer is located. Observations showed that the laser pointers were around 250 pixel area at 1 meter distance. Hence an area size range of 15 to 400 pixels is selected. Figure 3(c) shows the binary image after area threshold is applied.

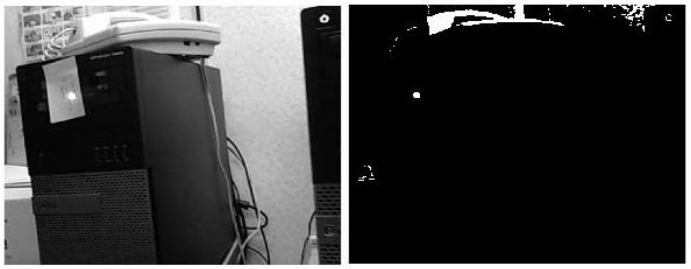

(a) Green channel image. **(b) Intensity threshold binary image.**

(c) Area threshold (ROI). **(d) Circular blob ROI.**

Fig. 3. Blob analysis for ROI.

In the final step an isoperimetric quotient is used to establish blob circularity (BC) in order to further narrow down the number of ROI obtained because laser pointer blobs tend to form a circular shape. Equation (1) was used to determine circularity.

$$f_{circle} = \frac{4\pi A}{P^2} \quad (1)$$

where A and P represent area and perimeter, respectively. A value of 1 means a perfect circle. Most blobs are not perfect circles. A threshold value of 0.7 ensures circularity while maintain a good error margin. Figure 3(d) shows ROI after circularity threshold is applied. The centroids of the final ROI are used to extract laser location by linear regression classification.

3.2. Laser intensity profile comparison

The final step of the algorithm evaluates ROI in the original image to pinpoint the location of laser pointer if present in the image. Uniform gradation is seen in the intensity plane of the laser point image and is symmetric across. The profile of the laser pointer, if affected by illumination variation, remains symmetric because the laser point image is small (approx. 250 pixel area given distance from camera is 1 meter). To classify a region as laser pointer, profiles are taken originating at the center of the ROI and extending to a radius of 20 pixels at 45 degree angles. Figure 4 shows an example of a laser spot with lines along which profiles are taken on a laser point across which pixel values are recorded to obtain profiles.

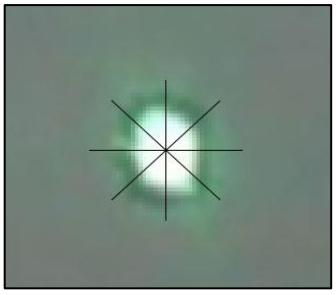

Fig. 4. Line segments on a laser point.

Figure 5 shows the color intensity profile of laser spot regions where the profiles are identified by angles. Figure 6 shows the intensity profile of ROI that are without a laser.

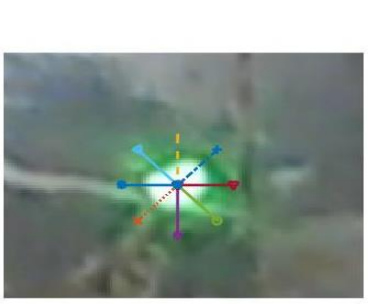

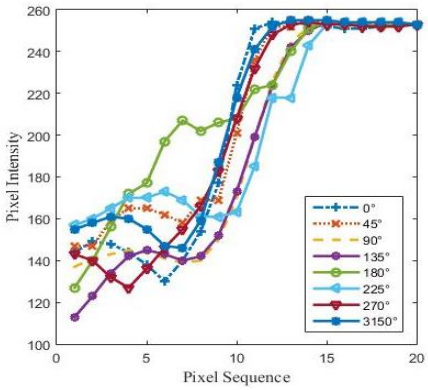

Fig. 5. Laser spot with intensity profile lines and the corresponding intensity profiles identified by angles.

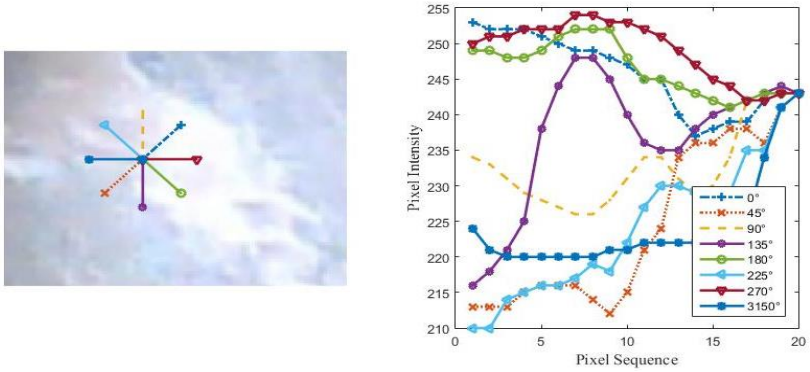

Fig. 6. Non-Laser ROI with intensity profile lines and the corresponding intensity profiles identified by angles.

The laser point intensity profiles are similar and comparable. Linear regression (LR) analysis and goodness of fit was used to establish the similarity. r^2, a fractional value between 0 and 1, indicates how well data fits into a statistical model, 1 being the best fit. Since all data sets, i.e., the intensity values along profiles, are similar when plotted against each other the deviation between them should be minimal. Deviation in this case represents the distance to linear model line and the actual points [23]. For data points represented by y_i and predictive model line represented byf_i, r^2 is given by

$$r^2 = 1 - \frac{SS_{res}}{SS_{tot}} \tag{2}$$

where SS_{res} and SS_{tot} are the residual and total sum of squares or sum of squared deviations and are defined by equations 3 and 4 respectively.

$$SS_{res} = \sum_i (y_i - f_i)^2 \tag{3}$$

where SS_{tot} is the total sum of squares of differences of each observation from the overall mean.

$$SS_{tot} = \sum_i (y_i - \bar{y})^2 \tag{4}$$

where $\bar{y}$ represents the mean of y_i

Pairs of opposite profiles are first compared. An average of r^2 values is taken. If there is one ROI then the r^2 value is checked. If the value is beyond a threshold of 0.7 then the ROI is classified as laser. In case of more than one ROI, the highest r^2 is analyzed. The threshold for r^2 is obtained experimentally and is discussed in Section 4. Figure 7 shows a regression analysis of the laser profiles and Fig. 8 shows regression analysis of non-laser profiles. The r^2 value of laser point is higher than non-laser candidates. A summarised Pseudo code of complete detection process is shown in Table 1.

4. Experimental Setup

At present there is no public database to assess the performance of laser pointer detection algorithm. For this study we obtained images in a lab environment with a laser pointer and camera being held an approximated 1 meter distance. The

experiment was conducted on a database consisting of 200 images out of which 107 images included laser point and the rest without laser point. The images were taken under uncontrolled illumination to incorporate the expected obstructions and challenges of a natural indoor environment as well as non-ideal laser pointer images cause by laser temporal movement. The laser pointer was aimed at surfaces of different reflection properties to make the database. The accuracy of the algorithm was also tested on a video of laser movement in 604 consecutive frames. The frame grabbing algorithm acquires frames at 15 fps.

The hardware used consists of a standard 1.3 MP web camera. The camera acquires images and video frames as RGB images of size 1024x1280 (90 dpi). The laser pointer used was green, *class III* laser with maximum power 5 mW and wave length of 532 nm. The algorithm was analysed using a basic dell optiplex7010 computer. The software used to develop the algorithm was MATLAB r2013a.

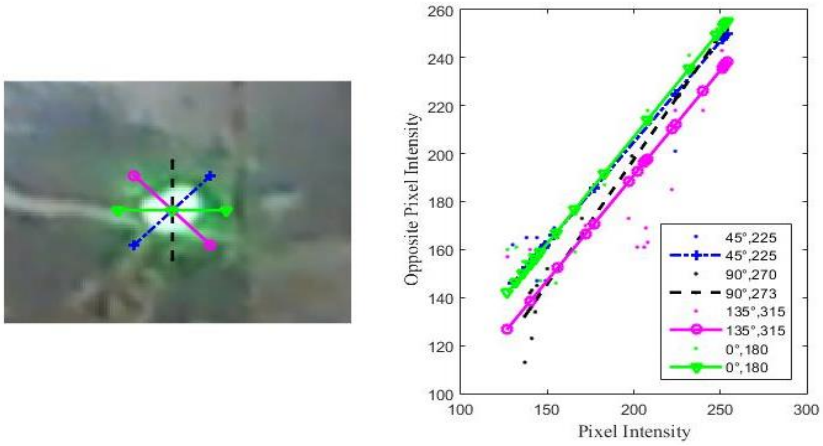

Fig. 7. Laser ROI and corresponding regression analysis of intensity profile. Regression points and pair of profiles compared are identified by angles. (Avg r^2 = 0.9132).

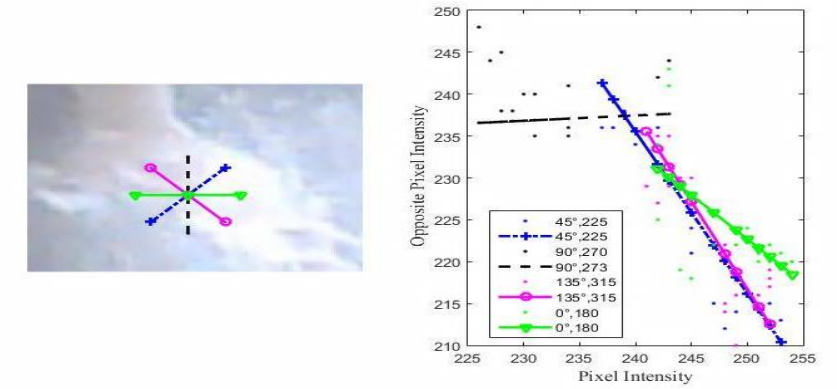

Fig. 8. Non Laser ROI and corresponding regression analysis of intensity profile. Regression points and pair of profiles compared are identified by angles. (Avg r^2 = 0.3123).

Table 1. Summarised Pseudo code of algorithm.

```
Initialise filter,
thresholdIntensity,thresholdArea,thresholdCircle,thres
holdRegression
0 input I,Image frame
1 I2=greenimage(I)
2 BinaryI=I2>thresholdI
3 Blobs=labeled connected areas(BinaryI)
4     If no Blob
5           No laser found
6     Return 0
7 BinaryI2=BinaryI(Blobs)>thresholdArea
8     If no Blob
9           No laser found
10    Return 0
11 MeasuresArea=area(Blobs)
12 MeasurePerimeter=perimeter(Blobs)
13 BlobCircularity=4*Pi*MeasuresArea/MeasurePerimeter
14 BinaryI3=BinaryI2(BlobCircularity)>thresholdCircle
15    If no Centroids found
16          No laser found
17    Else  Centroids= all Blob centroids
18       If Centroids found then
19          for allcentroids obtain
20                intensity profile pairs at angles:
21                            0,180
22                            45,225
23                            90,270
24                            135,315
25                Calculate RSS
26                Calculate TSS
27                PairRegressionValue=1-RSS/TSS
28                AvgRegressionValue
29        end
30    end
31          if  number centroid =1
32           AvgRegressionValue >thresholdRegression
33           laserCentroid = Centroid
34          elseif number of centroid >1
35           obtain maxRValue
36          if maxRegressionValue>thresholdRegression
37          laserCentroid=centroid(maxRValue)
38          else no laser
39          end
```

In order to evaluate the effectiveness of Linear Regression (LR) as a profile comparison measure, alternative data matching methods were used for classification. These variations are listed below:

- Bhattacharya distance (BD) [24]
- Euclidean distance (ED) [25]

- Standard deviation (SD), used in [8, 9]

Since Template matching (TM) based algorithms have shown high accuracy in [7, 8], TM was also used as alternative to blob analysis (BA+BC) for finding ROI. A template was obtained by averaging several laser pointer images. A high similarity region of laser pointer template in the image frame was obtained by normalized cross correlation (NCC). A detailed explanation of the method can be found in [26, 27]. The compared alternative methods based on TM are:

- Template Matching+Thresholding+Linear regression, i.e., (TM+T+LR).
- Template Matching+Thresholding Match Percentage, i.e (TM+MP).

The developed algorithm accuracy is also compared to video stream suitable methods described in [8, 7, 14]:

- Intensity Thresholding+Blob Area Thresholding, i.e (T+BA)
- Intensity Thresholding +Blob Area Thresholding+Blob Circularity measure, i.e., (T+BA+BC)

The best value of r^2 was chosen based on the experiment. The threshold values of all other algorithms were similarly set by repeated trial and error experiments. The outcomes of the algorithm were assessed using execution time and by accuracy as described in equation 5.

$$Accuracy = \frac{TP+TN}{TN+FN+TP+FP} \quad (5)$$

where, *TP* is the true positive outcomes, *TN* is the true negative outcomes, *FN* is false negative outcomes and *FP* is false positive outcomes.

5. Results and Discussion

The basic challenge of camera saturation which hinders laser point detection is more complex for indoor natural environments due to glare, which commonly occurs as a result of refection of light on various surfaces. The results presented in this section demonstrate the developed algorithms performance in such conditions. A comparison to some of the existing methods described in Section 2 is also given.

In order to get the best results from the developed algorithm, the regression threshold value was adjusted to achieve the highest accuracy. Figure 9 shows a graph of accuracy vs. regression value threshold. The highest accuracy is between regression threshold value r^2 range of 0.6-0.7, with the highest being 0.7.

Lower values of regression threshold correspond to lesser similarity in the compared ROI profiles which consequently lead to lesser accuracy. The laser images are non-ideal and their illumination is not controlled. Therefore, a strict level of similarity threshold therefore is not appropriate and only results in reduced accuracy. The optimum threshold is the mid-range values which work the best for the database. If hardware filters are applied or illumination and surface textured are controlled the similarity threshold may be set higher.

The algorithm classifier comparison with other similarity measures is presented in Table 2. As seen in this table, linear regression as similarity measure for profiles shows an accuracy improvement of 13 percent over standard deviation (SD) and Bhattacharya distance (BD). Euclidean distance (ED) shows much lower accuracy.

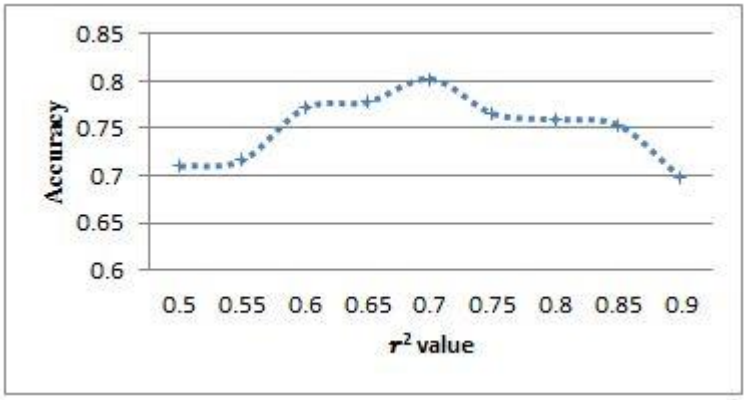

Fig. 9. Accuracy at different r^2values.

Table 2. Laser classifier accuracy.

Laser Classifier	Accuracy
BA+BC+T+BD	0.641
BA+BC+T+ED	0.586
BA+BC+T+SD	0.679
BA+BC+T+LR	**0.802**

A comparison of the accuracies for images as well as average time taken by each algorithm to complete one frame is presented in Table 3. The developed hybrid algorithm (T+BA+BC+LR) shows 8 times faster performance then the TM based version. It can be observed from the results that TM based algorithms have slower performance which would require high computing power for video based use. The developed algorithm has a runtime of 60 ms which implies that it takes about 60 ms for a 1024x1280 size image to be processed. This process time matches the frame rate of average cameras (15 fps) which matches the requisite of a standard real time processing. The experimentation was carried out with MATLAB software and the algorithm is estimated to run faster with more low level programing languages like C. The developed algorithm detects images with an accuracy of 80 percent which is a 20 percent improvement over all compared video compatible algorithms. This can be considered as a significant improvement, considering that detection was performed under natural indoor illumination, as most established detection approaches were not applied to such environments. Overall the developed hybrid algorithm shows improved accuracy with an acceptable processing time (0.061 s) in comparison to other approaches.

The algorithm performance was assessed using a continuous set of video frames and its result is consistent with the static results. To track a laser point in continuous frames, the search area was limited to a window over detected laser

position. Table 4 shows the comparison accuracies for the developed algorithm and various variations.

Table 3. Algorithm accuracy and runtime.

Algorithm	Detection accuracy	Average runtime
BA+BC+T+LR	0.8025	0.061
TM+T+LR	0.7963	0.527
TM+MP [20]	0.5556	0.493
BA+BC+T [19]	0.6481	0.060
T+BA [11]	0.3148	0.072

Table 4. Comparison of algorithm accuracies for continuous video frames.

Algorithm	Detection accuracy
BA+BC+T+LR	**0.980**
TM+T+LR	0.946
BA+BC+T	0.908
TM+MP	0.843
T+BA	0.793

From the table it can be observed that the accuracy of the developed algorithm in case of video has been increased to 98% making it an ideal candidate for use in a practical teleconsultation setup. Figure 10 shows a few frames averaged to describe a portion of the laser path from the video.

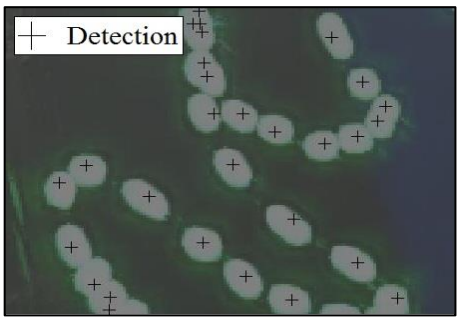

Fig. 10. Averaged consecutive video frames showing laser path.

6. Conclusion

This paper describes a hybrid algorithm combining thresholding, blob evaluation methods and profile similarity analysis by regression. The algorithm was tested on a database of 200 images which include images with and without a laser point and a video containing of 604 frames. The database was developed using no illumination control in natural indoor settings as such these images consist of glare among other challenging detection scenarios presented by different surfaces. Results show that the developed algorithm was able to perform at 20 percent higher accuracy in comparison with existing fast detection techniques, thus providing remarkable performance in terms of accuracy in natural indoor

environment. It is also observed that the developed algorithm is 8 times faster than template matching based approaches that are applied for natural environment laser pointer detection.

In conclusion, the developed algorithm shows high accuracy with low runtime and is hence ideal for real-time and practical applications. Additional hardware adjustments may improve the outcome, however the scope of this research is a completely software based solution to the laser pointer detection problem. This research is a preliminary stage in providing feedback setup for laser pointer assisted remote consultation. To further this research, a practical test in a remote consultation environment would be beneficial to assess additional requirements of the scenario.

Acknowledgment

This work has been supported by the Malaysian Ministry of Science, Technology and Innovation, MOSTI under grant 01-01-02-SF0882 and Universiti Kebangsaan Malaysia, DPP-2015-011.

References

1. DeJong, C.; Lucey, C.R.; and Dudley, R.A. (2015). Incorporating a new technology while doing no harm, Virtually. *Journal of the American Medical Association*, 314(22), 2351-2352.
2. Weinstein, R.S.; Lopez, A.M.; Joseph, B.A.; Erps, K.A.; Holcomb, M.; Barker, G.P.; and Krupinski, E.A. (2014). Telemedicine, telehealth, and mobile health applications that work: opportunities and barriers. *The American journal of medicine*, 127(3), 183-187.
3. Johansson, A.M.; Lindberg, I.; and Söderberg, S. (2014). Patients' Experiences with Specialist Care via Video Consultation in Primary Healthcare in Rural Areas. *International journal of telemedicine and application*, Volume 2014, Article ID 143824, 7 pages.
4. Mantas, J.; and Hasman, A. (2013). *Informatics, Management and Technology in Healthcare* (Vol. 190). IOS Press.
5. Kock, N. (2009). *E-Collaboration: Concepts, methodologies, tools, and applications* (1st ed.). IGI Global.
6. Karim, R.A.; Zakaria, N.F.; Zulkifley, M.A.; Mustafa, M.M.; Sagap, I.; and Latar, N.H. (2013). Telepointer technology in telemedicine: A review. *Biomedical engineering online*, 12(1), 1-19.
7. Matej, M.; and Toth, Š. (2013). Laser spot detection, *Journal of Information, Control and Management Systems*, 11 (1), 35-42.
8. Chávez, F.; Fernández, F.; Gacto, M.J.; and Alcalá, R. (2012). Automatic laser pointer detection algorithm for environment control device systems based on template matching and genetic tuning of fuzzy rule-based systems. *International Journal of Computational Intelligence Systems*, 5(2), 368-386.
9. Chávez, F.; Fernández, F.; Alcalá, R.; Alcalá-Fdez, J.; Olague, G.; and Herrera, F. (2012). Hybrid laser pointer detection algorithm based on

template matching and fuzzy rule-based systems for domotic control in real home environments. *Applied Intelligence*, 36(2), 407-423.

10. Widodo, R.B.; Chen, W.; and Matsumaru, T. (2012). Interaction using the projector screen and spot-light from a laser pointer: Handling some fundamentals requirements. *Proceedings of 2012 SICE Annual Conference (SICE), IEEE*, Akita, Japan, 1392-1397.
11. Kim, N.W.; Lee, S.J.; Lee, B.G.; and Lee, J.J. (2007). Vision based laser pointer interaction for flexible screens. *Proceedings of the 12th international conference on human-computer interaction: interaction platforms and techniques, Springer*, Beijing, China**,** Volume 4551, 845-853.
12. Olsen Jr, D.R.; and Nielsen, T. (2001). Laser pointer interaction. *Proceedings of the SIGCHI conference on Human factors in computing systems, ACM*, Seattle, Washington, USA, 17-22.
13. Kirstein, C.; and Muller, H. (1998). Interaction with a projection screen using a camera-tracked laser pointer. *Proceedings of the 1998 Conference on MultiMedia Modeling, IEEE Computer Society*, Lausanne, Switzerland, 191-192.
14. Lapointe, J.F.; and Godin, G. (2005). On-screen laser spot detection for large display interaction. *International Workshop on Haptic Audio Visual Environments and their Applications, 2005, IEEE*, Ontario, Canada , 72-76.
15. Khan, I.; Bais, A.; Roth, P.M.; Akhtar, M.; and Asif, M. (2015). Self-calibrating laser-pointer's spotlight detection system for projection screen interaction. *Proceedings of 12th International Bhurban Conference on Applied Sciences and Technology (IBCAST). IEEE*, Islamabad, Pakistan. 175-180.
16. Brown, M.S.; and Wong, W.K. (2003). Laser pointer interaction for camera-registered multiprojector displays. *Proceedings of the 2003 International Conference on Image Processing, ICIP, IEEE*, Barcelona, Spain, Volume 1, I-913-916.
17. Davis, J.; and Chen, X. (2002). Lumipoint: Multi-user laser-based interaction on large tiled displays. *Displays*, 23(5), 205-211.
18. Wada, T.; Takahashi, M.; Kagawa, K.; and Ohta, J. (2007). Laser pointer as a mouse. *Proceedings of the 2007 SICE Annual Conference, IEEE*, Kagawa, Japan, 369-372.
19. Vogt, F.; Wong, J.; Fels, S.; and Cavens, D. (2003). Tracking multiple laser pointers for large screen interaction. *Extended Abstracts of ACM UIST*, Volume 1, 95-96.
20. Widodo, R.B.; Chen, W.; and Matsumaru, T. (2012). Laser Spotlight Detection and Interpretation of Its Movement Behavior in Laser Pointer Interface. *Proceedings of the 2012 SICE International Symposium on System Integration, IEEE*, Fukuoka, Japan, 780-785.
21. Ahlborn, B.A.; Thompson, D.; Kreylos, O.; Hamann, B.; and Staadt, O.G. (2005). A practical system for laser pointer interaction on large displays. *Proceedings of the 2005 Symposium on Virtual reality software and technology , ACM*, Monterey, California, USA, 106-109.
22. Kemp, C.C.; Anderson, C.D.; Nguyen, H.; Trevor, A.J.; and Xu, Z. (2008). A point-and-click interface for the real world: laser designation of objects for

mobile manipulation. *Proceedings of the 2008 3rd ACM/IEEE International Conference on Human-Robot Interaction, IEEE*, Amsterdam, Netherlands, 241-248.

23. Chatterjee, S.; and Hadi, A.S. (2015). *Regression analysis by example* (5th ed.). John Wiley & Sons.
24. Aherne, F.J.; Thacker, N.A.; and Rockett, P.I. (1998). The Bhattacharyya metric as an absolute similarity measure for frequency coded data. *Kybernetika*, 34(4), 363-368.
25. Wang, L.; Zhang, Y.; and Feng, J. (2005). On the Euclidean distance of images. *IEEE Transactions on Pattern Analysis and Machine Intelligence*, 27(8), 1334-1339.
26. Lewis, J.P. (1995). Fast normalized cross-correlation. *Vision interface*, 10(1), 120-128.
27. Tsai, D.M.; and Lin, C.T. (2003). Fast normalized cross correlation for defects detection. *Pattern Recognnition Letters*, 24(15), 2625-2631.